

OPEN ACCESS

EDITED BY

Heng Liu,
Guangxi University for
Nationalities, China

REVIEWED BY

Guangming Xue,
Guangxi University of Finance and
Economics, China
Shumin Ha,
Shaanxi Normal University, China

*CORRESPONDENCE

Chenhui Wang
chwang@xmut.edu.cn;
wch0516@163.com

SPECIALTY SECTION

This article was submitted to
Dynamical Systems,
a section of the journal
Frontiers in Applied Mathematics and
Statistics

RECEIVED 10 February 2022

ACCEPTED 26 October 2022

PUBLISHED 22 November 2022

CITATION

Wang C (2022) Adaptive composite
learning dynamic surface control for
chaotic fractional-order permanent
magnet synchronous motors.
Front. Appl. Math. Stat. 8:1059756.
doi: 10.3389/fams.2022.1059756

COPYRIGHT

© 2022 Wang. This is an open-access
article distributed under the terms of
the [Creative Commons Attribution
License \(CC BY\)](https://creativecommons.org/licenses/by/4.0/). The use, distribution
or reproduction in other forums is
permitted, provided the original
author(s) and the copyright owner(s)
are credited and that the original
publication in this journal is cited, in
accordance with accepted academic
practice. No use, distribution or
reproduction is permitted which does
not comply with these terms.

Adaptive composite learning dynamic surface control for chaotic fractional-order permanent magnet synchronous motors

Chenhui Wang*

School of Mathematics and Statistics, Xiamen University of Technology, Xiamen, China

This paper aims to address the tracking problem of uncertain fractional-order permanent magnet synchronous motors with parametric uncertainties. To guarantee the system stability and offset the effect of parametric uncertainties, an adaptive backstepping composite learning neural control scheme based on interval excitation is presented. Moreover, dynamic surface technique is exploited to overcome the technical limitation of “explosion of complexity” caused by standard backstepping framework. In virtue of stability analysis and illustrative simulation, it is confirmed that the proposed control scheme not only attenuates the tracking error as small as possible, but also achieves satisfactory parametric convergence with high estimation precision.

KEYWORDS

fractional-order permanent magnet synchronous motors, composite learning, dynamic surface control, backstepping control, radial-basis-function neural networks

1. Introduction

Fractional calculus is an important mathematical discipline with a history of several centuries. In recent decades, fractional differential equations have made great progress in engineering, mechanics, physics, chemistry, and many other fields. Compared with classical mathematical models governed by integer-order differential equations, most fractional-order models have abundant advantages in describing the memory and genetic characteristics of the process [1, 2]. In addition, owing to the particularity of fractional calculus, fractional-order systems always exhibit rich dynamic behaviors [3–8].

Permanent magnet synchronous motor (PMSM) [9] has a great deal of advantages such as low production cost, high energy consumption, strong robustness, compact structure, superior performance, high inertia torque ratio, large power capacity. The

existing results show that integer-order PMSM has chaotic characteristics under some certain operating conditions. So far, several chaos control methods [10–14] have been put forward to attenuate the effect of chaotic oscillation and maintain the stable operation of integer-order PMSM. Fractional order PMSM [15–18] reflects the same complex chaotic dynamics, because fractional calculus provides a powerful tool for describing the genetic and infinite memory properties of different substances more accurately and essentially. Thus, the establishment of a chaos control scheme for fractional-order PMSM instead of the traditional one is of vast significance.

Radial basis function network (RBFNN) [19] has been widely concerned and applied due to its valuable characteristics of approximation for coping with functional uncertainty in controlled systems. The approximation ability of RBFNNs can greatly reduce the difficulty of modeling procedure in practical control problems and hence facilitates to simplify the controller design. Although a majority of the existing neural control approaches facilitates to realize error convergence, the approximation abilities of RBFNNs are generally restricted for the reason that the persistent excitation (PE) condition [20] must be met during the overall adaptation process. Actually, the PE condition for the implementation of traditional adaptive neural control is very strict and sometimes even infeasible in practical applications. In Wang and Hill [21], a neural control method based on a practical PE condition was proposed to guarantee the exponential stability of the closed-loop system as well as the exact approximation of RBFNNs. However, the parametric convergence rate *via* such a learning-based neural control method or its outgrowths (e.g., [22–24]) is highly dependent on the strength of PE, which may lead to very slow learning speed in general. Aiming to overcome this limitation, several scholars put forward useful composite learning control strategies [25–30]. Composite learning significantly relaxes the PE condition into the interval excitation (IE) condition. The essential idea of this method is to synthesize the online data and the historical data for the generation of a so-called prediction error and then to configure a composite adaptive law integrated with the tracking error and the prediction error for the better update of adaptive parameters.

Based on the above theoretical background, this paper studies the tracking issue of fractional-order PMSM. A neural network-based adaptive composite learning control approach is proposed, which can accurately estimate unknown functions under certain parameter design conditions. It will be proven that expected tracking performance and fast parametric convergence are realized once the proposed method is applied.

The main innovations of this work are worthy of emphasis as 2-fold: (1) Relying on fractional-order Lyapunov stability criterion, a novel fractional-order adaptive neural-network chaos controller is constructed to achieve robust tracking performance. Compared with the existing researches [10–14] on

integer-order PMSM, the tracking control problem of fractional-order PMSM dynamic model studied in the article is more challenging and significant due to the memory and genetic characteristics of fractional calculus. (2) A composite learning algorithm is proposed. Different from the conventional adaptive control methods [15–18] under the PE condition for fractional-order PMSM, the proposed composite learning adaptive control method relaxes the stringer PE condition into the IE condition which is relatively easy to be implemented. It will be proven that the designed composite learning algorithm not only updates the adaptive parameters of RBFNNs *via* taking advantage of the online data, but also effectively promote the estimation accuracy of all unknown functions.

The architecture of this article is organized as below. In Section 2, the fundamental background of fractional calculus, radial basis function network, persistent excitation, and interval excitation are recalled. Section 3 describes the considered problem formulation, and then, an adaptive neural-network controller based on composite learning scheme is systematically elaborated. It is verified that the proposed method facilitates to achieve satisfactory tracking performance and highly accurate parametric estimation under interval excitation condition. In Section 4, a numerical simulation is carried out to evaluate the feasibility of the proposed approach. In Section 5, the whole conclusion of the paper and the prospect of future research are summarized.

2. Preliminaries

2.1. Fractional calculus

In this overall article, \mathbb{N} (resp. \mathbb{R} , \mathbb{R}^n , \mathbb{R}^+ , \mathbb{C}) means the family of all non-zero natural numbers (resp. real numbers, n dimensional real vectors, positive numbers, complex numbers). Given a $k \in \mathbb{N}$, C^k is the family of all differentiable functions with continuous i -order derivatives for all $i = 1, 2, \dots, k$. L_∞ denotes the space of all bounded signals. $\text{sign}(\cdot)$ expresses the signum function. The transpose of an $x \in \mathbb{R}^n$ is denoted by x^T . $\Omega_r \triangleq \{x \in \mathbb{R} : |x| \leq r, r \in \mathbb{R}^+\}$.

Definition 1. Podlubny [2] *The β -order Caputo fractional derivative for a given differentiable function $\varphi(t)$ is formulated by*

$${}_{t_0}D_t^\beta \varphi(t) = \frac{1}{\Gamma(k-\beta)} \int_{t_0}^t \frac{\varphi^{(k)}(s)}{(t-s)^{\gamma+1-k}} ds$$

with $k-1 \leq \beta < k$ in which $k \in \mathbb{N}$. When $t_0 = 0$, we write $D^\beta \varphi(t)$ simply instead of ${}_{t_0}D_t^\beta \varphi(t)$.

Definition 2. Podlubny [2] *A mapping $E_{\beta,\gamma} : \mathbb{C} \rightarrow \mathbb{C}$ with double parameters $\beta, \gamma \in \mathbb{R}^+$ is called the Mittag-Leffler function, defined as*

$$E_{\beta,\gamma}(z) = \sum_{k=0}^{\infty} \frac{z^k}{\Gamma(\beta k + \gamma)}, \quad \forall z \in \mathbb{C}.$$

Particularly, $E_{1,1}(z) = e^z$. Let $E_\beta(z) \triangleq E_{\beta,1}(z)$ whenever $\gamma = 1$.

Lemma 1. Podlubny [2] Given $\beta \in (0, 2)$, $\gamma \in \mathbb{R}$. For an arbitrary $z \in \mathbb{C}$, if the argument $\arg(z)$ satisfies

$$\theta \leq |\arg(z)| \leq \pi$$

with $\beta\pi/2 < \theta \leq \min\{\pi, \beta\pi\}$, then the value of $E_{\beta,\gamma}(z)$ is limited within the estimation range:

$$|E_{\beta,\gamma}(z)| \leq \frac{C}{1 + |z|},$$

where $C \in \mathbb{R}^+$ is a constant.

Lemma 2. Gong [4] Let $V(t)$ be a continuous nonnegative function. Suppose that

$$D^\beta V(t) \leq -\lambda V(t) + \rho,$$

where $\lambda > 0$, $\rho \geq 0$. Then

$$V(t) \leq V(0)E_\beta(-\lambda t^\beta) + \frac{M\rho}{\lambda},$$

where $M = \max\{1, C\}$, $C \in \mathbb{R}^+$ is defined as in Lemma 1.

Lemma 3. Podlubny [2] Let $x(t)$ and $y(t)$ be differentiable functions, $C \in \mathbb{R}$, $\beta \in (0, 1)$. Then (1) $D^\beta C = 0$. (2) $D^\beta (mx(t) + ny(t)) = mD^\beta x(t) + nD^\beta y(t)$, where $m, n \in \mathbb{R}$ are constants.

Lemma 4. Aguila-Camacho et al. [3] Let $x(t)$ be a differentiable function, $\beta \in (0, 1)$. Then

$$\frac{1}{2}D^\beta x^2(t) \leq x(t)D^\beta x(t).$$

2.2. Radial basis function network

Recall the notion of radial basis function network (RBFNN) [19]. An RBFNN is represented by

$$\hat{f}(\mathbf{x}(t)) = \Theta^T(t)\Psi(\mathbf{x}(t)), \tag{1}$$

where $\hat{f}(\mathbf{x}(t)) \in \mathbb{R}$ is referred to as the output of RBFNN, $\mathbf{x}(t) \in \mathbb{R}^n$ is referred to as the input of RBFNN, $\Theta(t) = [\theta_1(t), \dots, \theta_m(t)]^T \in \mathbb{R}^m$ is a weight vector with m being the number of neural nodes, and $\Psi(\mathbf{x}(t)) \in \mathbb{R}^m$ is a vector of radial basis functions, the j th coordinate $\psi_j(\mathbf{x}(t))$ of $\Psi(\mathbf{x}(t))$ is usually defined to be the Gaussian function, that is

$$\psi_j(\mathbf{x}(t)) = \exp\left[-\frac{1}{w_j^2}(\mathbf{x}(t) - \boldsymbol{\varsigma}_j)^T(\mathbf{x}(t) - \boldsymbol{\varsigma}_j)\right],$$

where $\boldsymbol{\varsigma}_j \in \mathbb{R}^n$ describes the center of the receptive field, $w_j \in \mathbb{R}^+$ means the width of $\psi_j(\mathbf{x}(t))$.

Lemma 5. Sanner and Slotine [19] For any continuous function $f(\mathbf{x}(t))$ defined over a compact set Ω_r and any small positive scalar $\bar{\epsilon}$, one can find an RBFNN, denoted by $\Theta^{*T}\Psi(\mathbf{x}(t))$, such that

$$\sup_{\mathbf{x}(t) \in \Omega_r} |f(\mathbf{x}(t)) - \Theta^{*T}\Psi(\mathbf{x}(t))| \leq \bar{\epsilon},$$

in which Θ^* is the optimal RBFNN parameter, described by

$$\Theta^* = \arg \min_{\Theta(t) \in \mathbb{R}^m} \left\{ \sup_{\mathbf{x}(t) \in \Omega_r} \left| f(\mathbf{x}(t)) - \Theta^T(t)\Psi(\mathbf{x}(t)) \right| \right\}.$$

Lemma 6. Kurdila et al. [20] Given an $\mathbf{x}(t) \in \mathbb{R}^n$. Then, there exists a positive scalar ψ irrelevant with $\mathbf{x}(t)$ such that the regressor $\Psi(\mathbf{x}(t))$ defined in Equation (1) satisfies $\max\{\|\Psi(\mathbf{x}(t))\|, \|\Psi(\dot{\mathbf{x}}(t))\|\} \leq \psi$.

Definition 3. Pan et al. [25] Let $\mu > 0$ be an excitation strength and $\tau_0 > 0$ be a time duration. A time-varying vector $\Psi(t)$ is said to be of persistent excitation (PE), provided that $\int_{t-\tau_0}^t \Psi^T(\tau)\Psi(\tau)d\tau \geq \mu \mathbf{I}_{m \times m}$ for all $t > \tau_0$, where $\mathbf{I}_{m \times m}$ is an $m \times m$ unit matrix.

Definition 4. Pan et al. [25] Let $\mu > 0$ be an excitation strength and $\tau_0 > 0$ be a time duration. A time-varying vector $\Psi(t)$ is said to be of interval excitation (IE) over the interval $[T_e - \tau_0, T_e]$ with $T_e > \tau_0$, if $\int_{T_e - \tau_0}^{T_e} \Psi^T(\tau)\Psi(\tau)d\tau \geq \mu \mathbf{I}_{m \times m}$.

3. Main results

3.1. Problem formulation

Permanent magnet synchronous motor (PMSM) is a sort of special mechanical device whose dynamic behaviors manifest exclusive chaotic attractor. An integer-order PMSM dynamic system [10] can be modeled by

$$\begin{cases} \frac{d\omega}{dt} = \sigma(i_q - \omega), \\ \frac{di_q}{dt} = \gamma\omega - \omega i_d - i_q, \\ \frac{di_d}{dt} = u_d + \omega i_q - i_d, \end{cases} \tag{2}$$

where ω , i_d , and i_q symbolize the angular velocity, the d -axis current, and the q -axis current, respectively. σ and γ are two positive coefficients.

Put $\omega = x_1$, $i_q = x_2$ and $i_d = x_3$ in Equation (2), respectively. By substituting the β -order derivative operator $D^\beta(\cdot)$ with $0 < \beta < 1$ for $\frac{d(\cdot)}{dt}$, we generalize the aforesaid formulation into an uncertain fractional-order PMSM dynamic system in the state-space form as follows:

$$\begin{cases} D^\beta x_1(t) = f_1(\bar{\mathbf{x}}_1) + \sigma(x_2(t) - x_1(t)), \\ D^\beta x_2(t) = f_2(\bar{\mathbf{x}}_2) + \gamma x_1(t) - x_1(t)x_3(t) - x_2(t), \\ D^\beta x_3(t) = f_3(\bar{\mathbf{x}}_3) + u_d(t) + x_1(t)x_2(t) - x_3(t), \\ y(t) = x_1(t), \end{cases} \tag{3}$$

where $\bar{x}_i = [x_1, \dots, x_i]^T \in \mathbb{R}^i$ ($i = 1, 2, 3$) is a measurable state vector, $f_i: \mathbb{R}^i \rightarrow \mathbb{R}$ ($i = 1, 2, 3$) is an unknown bounded continuous nonlinear function, $y(t) \in \mathbb{R}$ is the system output, and $u_d(t) \in \mathbb{R}$ is the control input.

Let the initial values be $x_1(0) = x_2(0) = x_3(0) = 0.8$. When $\beta = 0.98$, $\sigma = 3$, and $\gamma = 30$, the chaotic attractor appears in the dynamic behaviors of fractional-order PMSM, see Figure 1.

The system controller will be designed in the next subsection such that the output signal $y(t)$ is driven to track the desired signal $y_d(t)$. To accomplish this tracking task, one needs to invoke the following assumption.

Assumption 1. Both of the signals $y_d(t)$ and $\mathcal{D}^\beta y_d(t)$ are known, bounded and smooth.

3.2. Control design

Next, let us expound the backstepping control design process for fractional-order PMSM.

Denote the virtual inputs by $\alpha_1(t)$ and $\alpha_2(t)$ for the first subsystem and the second subsystem, respectively. Let $\alpha_1(t)$ and $\alpha_2(t)$ pass the following fractional-order dynamic surfaces

$$\mathcal{D}^\beta \alpha_{i,c}(t) = -\varphi_i(\alpha_{i,c}(t) - \alpha_i(t)), \quad i = 1, 2 \quad (4)$$

respectively, where $\varphi_i \in \mathbb{R}^+$ are given constants, and the filter outputs $\alpha_{i,c}(t)$ satisfy the initial conditions $\alpha_{i,c}(0) = \alpha_i(0)$. Suppose that the parameters φ_i are selected suitably large. According to Liu et al. [27, Lemma 3], there are constants $\zeta_i \in \mathbb{R}^+$ such that $|\alpha_{i,c}(t) - \alpha_i(t)| \leq \zeta_i$ for all $t \geq 0$.

Consider the following coordinate translation:

$$e_1(t) = x_1(t) - y_d(t), \quad (5)$$

$$e_{i+1}(t) = x_{i+1}(t) - \alpha_{i,c}(t) \quad \text{for } i = 1, 2. \quad (6)$$

In light of Lemma 5, the existence of optimal RBFNN parameters $\Theta_{f_i}^*$ for $i = 1, 2, 3$ is guaranteed so that

$$f_i(\bar{x}_i) = \Theta_{f_i}^{*T} \Psi_{f_i}(\bar{x}_i) + \varepsilon_{f_i}(t), \quad i = 1, 2, 3 \quad (7)$$

respectively, in which $\varepsilon_{f_i}(t)$ represents the approximation error variable, which satisfies $|\varepsilon_{f_i}(t)| \leq \bar{\varepsilon}_i$ for some given scalar $\bar{\varepsilon}_i \in \mathbb{R}^+$. The parametric estimation error is taken as $\tilde{\Theta}_{f_i}(t) = \hat{\Theta}_{f_i}(t) - \Theta_{f_i}^*$.

Step 1. From Equations (3) and (7), it holds

$$\mathcal{D}^\beta x_1(t) = \Theta_{f_1}^{*T} \Psi_{f_1}(\bar{x}_1) + \varepsilon_{f_1}(t) + \sigma(x_2(t) - x_1(t)). \quad (8)$$

Hence, owing to Equations (5), (6), and (8), computing the fractional time derivative of $e_1(t)$ yields

$$\begin{aligned} \mathcal{D}^\beta e_1(t) &= \mathcal{D}^\beta x_1(t) - \mathcal{D}^\beta y_d(t) \\ &= f_1(\bar{x}_1) + \sigma(x_2(t) - x_1(t)) - \mathcal{D}^\beta y_d(t) \\ &= f_1(\bar{x}_1) + (\sigma - 1)(x_2(t) - x_1(t)) + (x_2(t) - \alpha_{1,c}(t)) \\ &\quad + (\alpha_{1,c}(t) - \alpha_1(t)) + (\alpha_1(t) - x_1(t)) - \mathcal{D}^\beta y_d(t) \quad (9) \\ &= \hat{\Theta}_{f_1}^T(t) \Psi_{f_1}(\bar{x}_1) - \tilde{\Theta}_{f_1}^T(t) \Psi_{f_1}(\bar{x}_1) \\ &\quad + \varepsilon_{f_1}(t) + (\sigma - 1)(x_2(t) - x_1(t)) + e_2(t) + z_1(t) \\ &\quad + \alpha_1(t) - x_1(t) - \mathcal{D}^\beta y_d(t), \end{aligned}$$

where $z_1(t) = \alpha_{1,c}(t) - \alpha_1(t)$ is the filter error.

The virtual control function for the first subsystem is defined by

$$\begin{aligned} \alpha_1(t) &= -k_1 e_1(t) - \hat{\Theta}_{f_1}^T(t) \Psi_{f_1}(\bar{x}_1) - (\sigma - 1)(x_2(t) - x_1(t)) \\ &\quad + x_1(t) - e_1(t) + \mathcal{D}^\beta y_d(t), \end{aligned} \quad (10)$$

where k_1 is a positive known constant.

Incorporating Equation (10) into Equation (9) infers

$$\begin{aligned} \mathcal{D}^\beta e_1(t) &= -\tilde{\Theta}_{f_1}^T(t) \Psi_{f_1}(\bar{x}_1) + \varepsilon_{f_1}(t) - k_1 e_1(t) \\ &\quad + e_2(t) - e_1(t) + z_1(t). \end{aligned} \quad (11)$$

It is worth noting that $|z_1(t)| \leq \zeta_1$. By Young inequality, multiplying both sides of Equation (11) by $e_1(t)$ induces

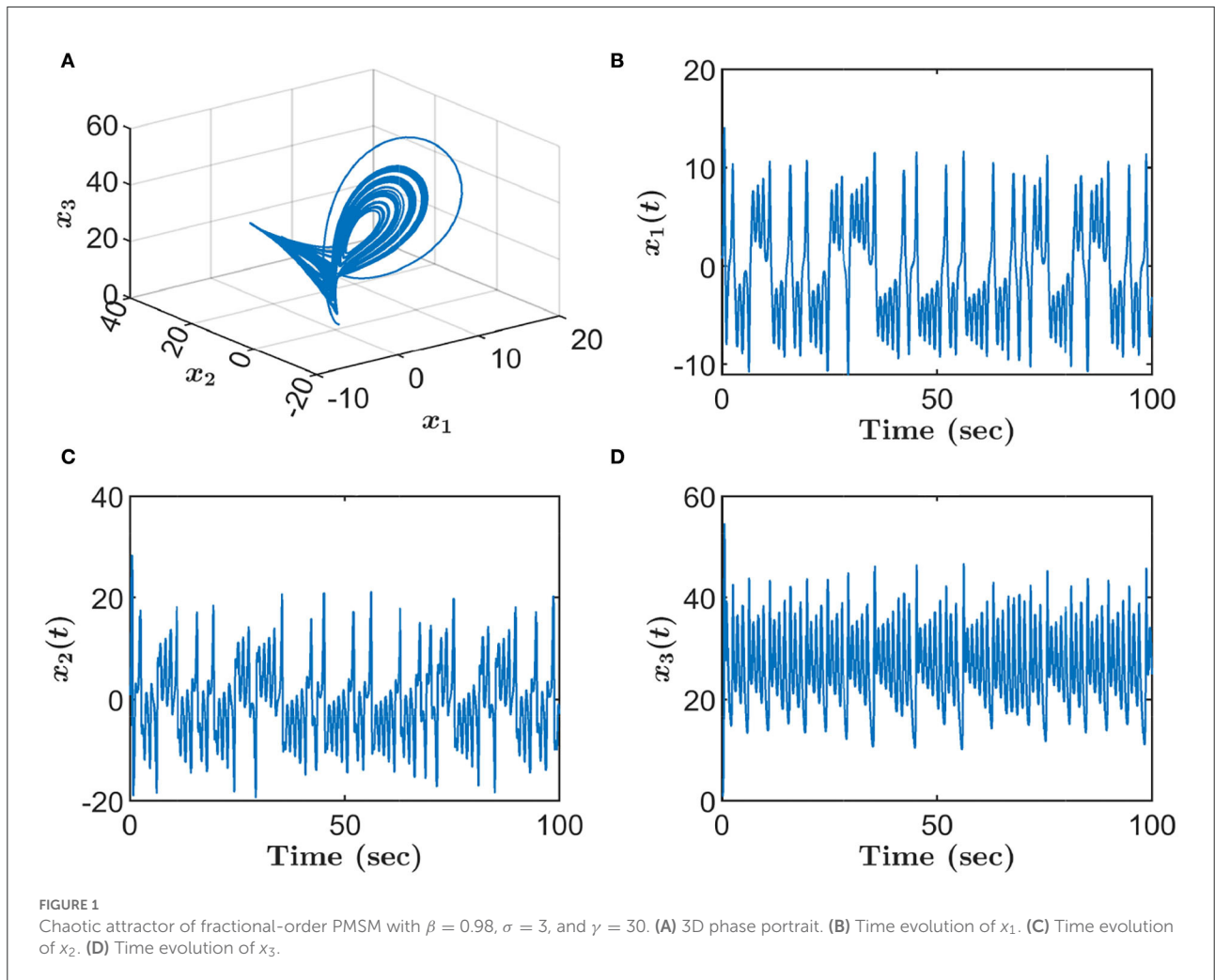
$$\begin{aligned} e_1(t) \mathcal{D}^\beta e_1(t) &= -e_1(t) \tilde{\Theta}_{f_1}^T(t) \Psi_{f_1}(\bar{x}_1) + e_1(t) \varepsilon_{f_1}(t) \\ &\quad - k_1 e_1^2(t) + e_1(t) e_2(t) - e_1^2(t) + e_1(t) z_1(t) \\ &\leq -e_1(t) \tilde{\Theta}_{f_1}^T(t) \Psi_{f_1}(\bar{x}_1) + \frac{1}{2} e_1^2(t) + \frac{1}{2} \varepsilon_{f_1}^2(t) \\ &\quad - k_1 e_1^2(t) + e_1(t) e_2(t) - e_1^2(t) + \frac{1}{2} e_1^2(t) + \frac{1}{2} \zeta_1^2 \\ &= -e_1(t) \tilde{\Theta}_{f_1}^T(t) \Psi_{f_1}(\bar{x}_1) - k_1 e_1^2(t) + e_1(t) e_2(t) \\ &\quad + \frac{1}{2} \varepsilon_{f_1}^2 + \frac{1}{2} \zeta_1^2. \end{aligned} \quad (12)$$

In general, the traditional adaptation law can only make sure that the parametric estimation error $\tilde{\Theta}_{f_i}(t)$ is bounded under the PE condition. However, the PE condition is sometimes too stringent to be fulfilled, and thus, satisfactory parametric convergence cannot be ensured. Motivated by this reason, a composite learning approach will be studied in the sequel to achieve higher precision of $\hat{\Theta}_{f_i}(t)$ with the removal of the rigorous PE condition.

Define a mapping $\mathbf{m}_1: [0, +\infty) \rightarrow \mathbb{R}^{m \times m}$ by

$$\mathbf{m}_1(t) = \int_{t-\tau_1}^t \Psi_{f_1}(\bar{x}_1(\tau)) \Psi_{f_1}^T(\bar{x}_1(\tau)) d\tau,$$

where $\tau_1 > 0$ is a certain integration duration.



Suppose that $\mathbf{m}_1(t) \geq \mu_1 \mathbf{I}$ with $\mu_1 > 0$ standing for the exciting strength, whenever $\Psi_{f_1}(\bar{\mathbf{x}}_1(t))$ is of IE on $t \in [T_{e_1} - \tau_1, T_{e_1}]$ for a time instant $T_{e_1} > \tau_1$. Take into account the next prediction error defined by

$$\hat{\mathbf{e}}_1(t) = \begin{cases} \mathbf{m}_1(t)\tilde{\Theta}_{f_1}(t) - \tilde{\mathbf{e}}_{f_1}(t), & t < T_{e_1} \\ \mathbf{m}_1(t)\tilde{\Theta}_{f_1}(T_{e_1}) - \tilde{\mathbf{e}}_{f_1}(T_{e_1}), & t \geq T_{e_1} \end{cases} \quad (13)$$

where $\tilde{\mathbf{e}}_{f_1} : [0, +\infty) \rightarrow \mathbb{R}^{m \times 1}$ is expressed as

$$\tilde{\mathbf{e}}_{f_1}(t) = \int_{t-\tau_1}^t \Psi_{f_1}(\bar{\mathbf{x}}_1(\tau)) \varepsilon_{f_1}(\tau) d\tau.$$

The fractional-order composite learning adaptation law is designed as

$$\mathcal{D}^\beta \hat{\Theta}_{f_1}(t) = \varrho_1 e_1(t) \Psi_{f_1}(\bar{\mathbf{x}}_1(t)) - \eta_1 \hat{\Theta}_{f_1}(t) - \varrho_1 \varpi_1 \hat{\mathbf{e}}_1(t), \quad (14)$$

where ϱ_1, η_1 , and $\varpi_1 \in \mathbb{R}^+$ are known constants.

Construct an auxiliary variable $\mathbf{H}_1(t)$ by

$$\mathbf{H}_1(t) = \mathbf{m}_1(t)\Theta_{f_1}^* + \tilde{\mathbf{e}}_{f_1}(t). \quad (15)$$

Apparently, it is observed from Equation (8) that

$$\Theta_{f_1}^{*T} \Psi_{f_1}(\bar{\mathbf{x}}_1) + \varepsilon_{f_1}(t) = \mathcal{D}^\beta x_1(t) - \sigma(x_2(t) - x_1(t)). \quad (16)$$

Multiply both sides of Equation (16) by $\Psi_{f_1}(\bar{\mathbf{x}}_1)$. Then, it is inferred that

$$\begin{aligned} & \Psi_{f_1}(\bar{\mathbf{x}}_1) \left[\Psi_{f_1}^T(\bar{\mathbf{x}}_1) \Theta_{f_1}^* + \varepsilon_{f_1}(t) \right] \\ &= \Psi_{f_1}(\bar{\mathbf{x}}_1) \left[\mathcal{D}^\beta x_1(t) - \sigma(x_2(t) - x_1(t)) \right]. \end{aligned} \quad (17)$$

Invoking Equations (15) and (17), we can gain access to the precise value of $\mathbf{H}_1(t)$ as

$$\mathbf{H}_1(t) = \int_{t-\tau_1}^t \Psi_{f_1}(\bar{\mathbf{x}}_1(\tau)) \left[\mathcal{D}^\beta x_1(\tau) - \sigma(x_2(\tau) - x_1(\tau)) \right] d\tau.$$

Consequently, the value of $\hat{\mathbf{e}}_1(t)$ can be acquired precisely as

$$\begin{aligned} \hat{\mathbf{e}}_1(t) &= \mathbf{m}_1(t)\hat{\Theta}_{f_1}(t) - \mathbf{m}_1(t)\Theta_{f_1}^* - \tilde{\mathbf{e}}_{f_1}(t) \\ &= \mathbf{m}_1(t)\hat{\Theta}_{f_1}(t) - \mathbf{H}_1(t). \end{aligned} \quad (18)$$

Substituting Equation (18) into Equation (14), one arrives at

$$\begin{aligned} \mathcal{D}^\beta \hat{\Theta}_{f_1}(t) &= \varrho_1 e_1(t) \Psi_{f_1}(\bar{\mathbf{x}}_1(t)) - \eta_1 \hat{\Theta}_{f_1}(t) \\ &+ \varrho_1 \varpi_1 (\mathbf{H}_1(t) - \mathbf{m}_1(t) \hat{\Theta}_{f_1}(t)). \end{aligned} \quad (19)$$

Consider the next quadratic Lyapunov function:

$$V_1(t) = \frac{1}{2} e_1^2(t) + \frac{1}{2\varrho_1} \tilde{\Theta}_{f_1}^T(t) \tilde{\Theta}_{f_1}(t). \quad (20)$$

Invoking Lemmas 3 and 4, simple manipulation on the fractional differentiation of Equation (20) renders

$$\begin{aligned} \mathcal{D}^\beta V_1(t) &= \frac{1}{2} \mathcal{D}^\beta e_1^2(t) + \frac{1}{2\varrho_1} \mathcal{D}^\beta (\tilde{\Theta}_{f_1}^T(t) \tilde{\Theta}_{f_1}(t)) \\ &\leq e_1(t) \mathcal{D}^\beta e_1(t) + \frac{1}{\varrho_1} \tilde{\Theta}_{f_1}^T(t) \mathcal{D}^\beta \tilde{\Theta}_{f_1}(t) \\ &= e_1(t) \mathcal{D}^\beta e_1(t) + \frac{1}{\varrho_1} \tilde{\Theta}_{f_1}^T(t) \mathcal{D}^\beta \hat{\Theta}_{f_1}(t). \end{aligned} \quad (21)$$

Application of Young's inequality gives

$$\begin{aligned} -\tilde{\Theta}_{f_1}^T(t) \hat{\Theta}_{f_1}(t) &= -\tilde{\Theta}_{f_1}^T(t) \Theta_{f_1}^* - \tilde{\Theta}_{f_1}^T(t) \tilde{\Theta}_{f_1}(t) \\ &\leq \frac{1}{2} \Theta_{f_1}^{*T} \Theta_{f_1}^* + \frac{1}{2} \tilde{\Theta}_{f_1}^T(t) \tilde{\Theta}_{f_1}(t) - \tilde{\Theta}_{f_1}^T(t) \tilde{\Theta}_{f_1}(t) \\ &= \frac{1}{2} \Theta_{f_1}^{*T} \Theta_{f_1}^* - \frac{1}{2} \tilde{\Theta}_{f_1}^T(t) \tilde{\Theta}_{f_1}(t). \end{aligned} \quad (22)$$

Moreover, by using Young's inequality and Lemma 6, it is shown that

$$\begin{aligned} \varpi_1 \tilde{\Theta}_{f_1}^T(t) \tilde{\Theta}_{f_1}(t) &\leq \frac{1}{2} \tilde{\Theta}_{f_1}^T(t) \tilde{\Theta}_{f_1}(t) + \frac{1}{2} \varpi_1^2 \tilde{\Theta}_{f_1}^T(t) \tilde{\Theta}_{f_1}(t) \\ &\leq \frac{1}{2} \tilde{\Theta}_{f_1}^T(t) \tilde{\Theta}_{f_1}(t) + \frac{1}{2} \varpi_1^2 \tilde{\Theta}_{f_1}^2 \\ &\quad \max_{\tau \in [t-\tau_1, t]} \|\Psi_{f_1}(\bar{\mathbf{x}}_1(\tau))\|^2 \left(\int_{t-\tau_1}^t d\tau \right)^2 \\ &\leq \frac{1}{2} \tilde{\Theta}_{f_1}^T(t) \tilde{\Theta}_{f_1}(t) + \frac{1}{2} (\varpi_1 \bar{\varepsilon}_1 \psi_1 \tau_1)^2 \end{aligned} \quad (23)$$

with $\psi_1 > 0$ being a constant which is independent of $\bar{\mathbf{x}}_1(t)$ and the number of neural nodes.

Considering Equations (12)–(14) and Equation (19)–(23), we conclude

$$\begin{aligned} \mathcal{D}^\beta V_1(t) &\leq -e_1(t) \tilde{\Theta}_{f_1}^T(t) \Psi_{f_1}(\bar{\mathbf{x}}_1) - k_1 e_1^2(t) + e_1(t) e_2(t) + \frac{1}{2} \zeta_1^2 + \frac{1}{2} \bar{\varepsilon}_1^2 \\ &\quad + \frac{1}{\varrho_1} \tilde{\Theta}_{f_1}^T(t) \left[\varrho_1 e_1(t) \Psi_{f_1}(\bar{\mathbf{x}}_1) - \eta_1 \hat{\Theta}_{f_1}(t) - \varrho_1 \varpi_1 \hat{\Theta}_{f_1}(t) \right] \\ &= -k_1 e_1^2(t) + e_1(t) e_2(t) - \frac{\eta_1}{\varrho_1} \tilde{\Theta}_{f_1}^T(t) \hat{\Theta}_{f_1}(t) \\ &\quad - \varpi_1 \tilde{\Theta}_{f_1}^T(t) \hat{\Theta}_{f_1}(t) + \frac{1}{2} \zeta_1^2 + \frac{1}{2} \bar{\varepsilon}_1^2 \\ &\leq -k_1 e_1^2(t) + e_1(t) e_2(t) - \frac{\eta_1}{2\varrho_1} \tilde{\Theta}_{f_1}^T(t) \tilde{\Theta}_{f_1}(t) \\ &\quad + \frac{\eta_1}{2\varrho_1} \Theta_{f_1}^{*T} \Theta_{f_1}^* + \frac{1}{2} \zeta_1^2 + \frac{1}{2} \bar{\varepsilon}_1^2 \\ &\quad - \varpi_1 \tilde{\Theta}_{f_1}^T(t) (\mathbf{m}_1(t) \tilde{\Theta}_{f_1}(t) - \tilde{\Theta}_{f_1}(t)) \\ &= -k_1 e_1^2(t) + e_1(t) e_2(t) - \frac{\eta_1}{2\varrho_1} \tilde{\Theta}_{f_1}^T(t) \tilde{\Theta}_{f_1}(t) + \frac{\eta_1}{2\varrho_1} \Theta_{f_1}^{*T} \Theta_{f_1}^* \\ &\quad - \varpi_1 \mu_1 \tilde{\Theta}_{f_1}^T(t) \tilde{\Theta}_{f_1}(t) + \varpi_1 \tilde{\Theta}_{f_1}^T(t) \tilde{\Theta}_{f_1}(t) + \frac{1}{2} \zeta_1^2 + \frac{1}{2} \bar{\varepsilon}_1^2 \\ &\leq -k_1 e_1^2(t) + e_1(t) e_2(t) - \frac{\eta_1 + \varrho_1 (2\varpi_1 \mu_1 - 1)}{2\varrho_1} \tilde{\Theta}_{f_1}^T(t) \tilde{\Theta}_{f_1}(t) \\ &\quad + \frac{\eta_1}{2\varrho_1} \Theta_{f_1}^{*T} \Theta_{f_1}^* + \frac{1}{2} (\varpi_1 \bar{\varepsilon}_1 \psi_1 \tau_1)^2 + \frac{1}{2} \zeta_1^2 + \frac{1}{2} \bar{\varepsilon}_1^2 \\ &\leq -a_1 V_1(t) + e_1(t) e_2(t) + b_1, \end{aligned} \quad (24)$$

where $a_1 = \min\{2k_1, \eta_1 + \varrho_1(2\varpi_1\mu_1 - 1)\}$, $b_1 = 0.5\varrho_1^{-1}\eta_1\|\Theta_{f_1}^*\|^2 + 0.5\varpi_1^2\bar{\varepsilon}_1^2\psi_1^2\tau_1^2 + 0.5\zeta_1^2 + 0.5\bar{\varepsilon}_1^2$.

Step 2. According to Equations (3) and (7), we have

$$\mathcal{D}^\beta x_2(t) = \Theta_{f_2}^{*T} \Psi_{f_2}(\bar{\mathbf{x}}_2) + \varepsilon_{f_2}(t) + \gamma x_1(t) - x_1(t)x_3(t) - x_2(t). \quad (25)$$

With the aid of Equations (6) and (25), we can derive

$$\begin{aligned} \mathcal{D}^\beta e_2(t) &= \mathcal{D}^\beta x_2(t) - \mathcal{D}^\beta \alpha_{1,c}(t) \\ &= f_2(\bar{\mathbf{x}}_2) - x_2(t) - x_1(t)x_3(t) + \gamma x_1(t) - \mathcal{D}^\beta \alpha_{1,c}(t) \\ &= \hat{\Theta}_{f_2}^T(t) \Psi_{f_2}(\bar{\mathbf{x}}_2) - \tilde{\Theta}_{f_2}^T(t) \Psi_{f_2}(\bar{\mathbf{x}}_2) + \varepsilon_{f_2}(t) \\ &\quad - x_2(t) - x_1(t)x_3(t) - x_1(t)z_2(t) - x_1(t)\alpha_2(t) \\ &\quad + \gamma x_1(t) - \mathcal{D}^\beta \alpha_{1,c}(t), \end{aligned} \quad (26)$$

where $z_2(t) = \alpha_{2,c}(t) - \alpha_2(t)$ is the filter error.

The virtual controller is provided as

$$\begin{aligned} \alpha_2(t) &= \frac{1}{x_1(t)} [k_2 e_2(t) + \frac{1}{2} (x_1^2(t) + 1) e_2(t) + \hat{\Theta}_{f_2}^T(t) \Psi_{f_2}(\bar{\mathbf{x}}_2) \\ &\quad - x_2(t) + \gamma x_1(t) + e_1(t) - \mathcal{D}^\beta \alpha_{1,c}(t)] \end{aligned} \quad (27)$$

with $k_2 > 0$ being a design parameter.

Substituting Equation (27) into Equation (26) induces

$$\begin{aligned} \mathcal{D}^\beta e_2(t) = & -k_2 e_2(t) - \frac{1}{2}(x_1^2(t) + 1)e_2(t) - \tilde{\Theta}_{f_2}^T(t)\Psi_{f_2}(\bar{\mathbf{x}}_2) \\ & + \varepsilon_{f_2}(t) - e_1(t) - x_1(t)z_2(t) - x_1(t)e_3(t). \end{aligned} \tag{28}$$

Multiply both sides of Equation (28) by $e_2(t)$. Employing Lemma 4 and Young inequality, we argue

$$\begin{aligned} e_2(t)\mathcal{D}^\beta e_2(t) = & -k_2 e_2^2(t) - \frac{1}{2}(x_1^2(t) + 1)e_2^2(t) \\ & - e_2(t)\tilde{\Theta}_{f_2}^T(t)\Psi_{f_2}(\bar{\mathbf{x}}_2) + e_2(t)\varepsilon_{f_2}(t) \\ & - x_1(t)e_2(t)e_3(t) - x_1(t)e_2(t)z_2(t) - e_1(t)e_2(t) \\ \leq & -k_2 e_2^2(t) - \frac{1}{2}(x_1^2(t) + 1)e_2^2(t) - e_2(t)\tilde{\Theta}_{f_2}^T(t) \\ & \Psi_{f_2}(\bar{\mathbf{x}}_2) + \frac{1}{2}e_2^2(t) + \frac{1}{2}\bar{\varepsilon}_2^2 - x_1(t)e_2(t)e_3(t) \\ & + \frac{1}{2}x_1^2(t)e_2^2(t) + \frac{1}{2}\zeta_2^2 - e_1(t)e_2(t) \\ \leq & -k_2 e_2^2(t) - e_2(t)\tilde{\Theta}_{f_2}^T(t)\Psi_{f_2}(\bar{\mathbf{x}}_2) - x_1(t)e_2(t)e_3(t) \\ & - e_1(t)e_2(t) + \frac{1}{2}\zeta_2^2 + \frac{1}{2}\bar{\varepsilon}_2^2. \end{aligned} \tag{29}$$

Let $\Psi_{f_2}(\bar{\mathbf{x}}_2(t))$ be of IE over the interval $[T_{e_2} - \tau_2, T_{e_2}]$ for some $\tau_2 > 0$ and $T_{e_2} > \tau_2$.

Define the following prediction error

$$\hat{\mathbf{e}}_2(t) = \begin{cases} \mathbf{m}_2(t)\tilde{\Theta}_{f_2}^T(t) - \tilde{\varepsilon}_{f_2}(t), & t < T_{e_2} \\ \mathbf{m}_2(t)\tilde{\Theta}_{f_2}^T(T_{e_2}) - \tilde{\varepsilon}_{f_2}(T_{e_2}), & t \geq T_{e_2} \end{cases} \tag{30}$$

where $\mathbf{m}_2 : [0, +\infty) \rightarrow \mathbb{R}^{m \times m}$ and $\tilde{\varepsilon}_{f_2} : [0, +\infty) \rightarrow \mathbb{R}^{m \times 1}$ are formulated by

$$\mathbf{m}_2(t) = \int_{t-\tau_0}^t \Psi_{f_2}(\bar{\mathbf{x}}_2(\tau))\Psi_{f_2}^T(\bar{\mathbf{x}}_2(\tau))d\tau,$$

and

$$\tilde{\varepsilon}_{f_2}(t) = \int_{t-\tau_2}^t \Psi_{f_2}(\bar{\mathbf{x}}_2(\tau))\varepsilon_{f_2}(\tau)d\tau,$$

respectively. Presume that $\mathbf{m}_2(t) \geq \mu_2 \mathbf{I}$, where μ_2 is the exciting strength.

Choose the composite learning-based adaptation law as below:

$$\mathcal{D}^\beta \hat{\Theta}_{f_2}^T(t) = \varrho_2 e_2(t)\Psi_{f_2}(\bar{\mathbf{x}}_2(t)) - \eta_2 \hat{\Theta}_{f_2}^T(t) - \varrho_2 \varpi_2 \hat{\mathbf{e}}_2(t), \tag{31}$$

where ϱ_2, η_2 , and ϖ_2 are given positive scalars.

Define the following auxiliary term:

$$\mathbf{H}_2(t) = \mathbf{m}_2(t)\Theta_{f_2}^* + \tilde{\varepsilon}_{f_2}(t). \tag{32}$$

On account of Equation (25), it is trivially seen that

$$\Theta_{f_2}^{*T}\Psi_{f_2}(\bar{\mathbf{x}}_2) + \varepsilon_{f_2}(t) = \mathcal{D}^\beta x_2(t) - \gamma x_1(t) + x_1(t)x_3(t) + x_2(t). \tag{33}$$

Multiply both sides of Equation (33) by $\Psi_{f_2}(\bar{\mathbf{x}}_2)$. Then, it is inferred that

$$\begin{aligned} & \Psi_{f_2}(\bar{\mathbf{x}}_2) \left[\Psi_{f_2}^T(\bar{\mathbf{x}}_2)\Theta_{f_2}^* + \varepsilon_{f_2}(t) \right] \\ = & \Psi_{f_2}(\bar{\mathbf{x}}_2) \left[\mathcal{D}^\beta x_2(t) - \gamma x_1(t) + x_1(t)x_3(t) + x_2(t) \right]. \end{aligned} \tag{34}$$

Due to Equations (32) and (34), the computational result of $\mathbf{H}_2(t)$ is attainable, that is

$$\mathbf{H}_2(t) = \int_{t-\tau_2}^t \Psi_{f_2}(\bar{\mathbf{x}}_2) \left[\mathcal{D}^\beta x_2(\tau) - \gamma x_1(\tau) + x_1(\tau)x_3(\tau) + x_2(\tau) \right].$$

Accordingly, the precise value of $\hat{\mathbf{e}}_2(t)$ is determined by

$$\hat{\mathbf{e}}_2(t) = \mathbf{m}_2(t)\hat{\Theta}_{f_2}^T(t) - \mathbf{H}_2(t).$$

Define the Lyapunov function by

$$V_2(t) = V_1(t) + \frac{1}{2}e_2^2(t) + \frac{1}{2\varrho_2}\tilde{\Theta}_{f_2}^T(t)\tilde{\Theta}_{f_2}(t). \tag{35}$$

By Lemmas 3 and 4, taking the fractional derivative of Equation (35) leads to

$$\begin{aligned} \mathcal{D}^\beta V_2(t) = & \mathcal{D}^\beta V_1(t) + \frac{1}{2}\mathcal{D}^\beta e_2^2(t) + \frac{1}{2\varrho_2}\mathcal{D}^\beta \tilde{\Theta}_{f_2}^T(t)\tilde{\Theta}_{f_2}(t) \\ \leq & \mathcal{D}^\beta V_1(t) + e_2(t)\mathcal{D}^\beta e_2(t) + \frac{1}{\varrho_2}\tilde{\Theta}_{f_2}^T(t)\mathcal{D}^\beta \tilde{\Theta}_{f_2}(t) \\ = & \mathcal{D}^\beta V_1(t) + e_2(t)\mathcal{D}^\beta e_2(t) + \frac{1}{\varrho_2}\tilde{\Theta}_{f_2}^T(t)\mathcal{D}^\beta \hat{\Theta}_{f_2}^T(t). \end{aligned} \tag{36}$$

Analogous to Equations (22) and (23), it is easily verified that

$$-\tilde{\Theta}_{f_2}^T(t)\hat{\Theta}_{f_2}^T(t) \leq -\frac{1}{2}\tilde{\Theta}_{f_2}^T(t)\tilde{\Theta}_{f_2}(t) + \frac{1}{2}\Theta_{f_2}^{*T}\Theta_{f_2}^*, \tag{37}$$

$$\varpi_2 \tilde{\Theta}_{f_2}^T(t)\tilde{\varepsilon}_{f_2}(t) \leq \frac{1}{2}\tilde{\Theta}_{f_2}^T(t)\tilde{\Theta}_{f_2}(t) + \frac{1}{2}(\varpi_2 \bar{\varepsilon}_2 \psi_2 \tau_2)^2, \tag{38}$$

in which $\psi_2 \geq \|\Psi_{f_2}(\bar{\mathbf{x}}_2(t))\|$ is a positive constant irrelevant with $\bar{\mathbf{x}}_2(t)$ and the number of neural nodes.

By means of Equations (29), (31), and (36)–(38), we get

$$\begin{aligned}
 & \mathcal{D}^\beta V_2(t) \\
 & \leq \mathcal{D}^\beta V_1(t) + e_2(t)\mathcal{D}^\beta e_2(t) + \frac{1}{2}\zeta_2^2 + \frac{1}{2}\bar{\varepsilon}_2^2 \\
 & \quad + \frac{1}{\varrho_2} \tilde{\Theta}_{f_2}^T(t) \left[\varrho_2 e_2(t) \Psi_{f_2}(\bar{\mathbf{x}}_2) - \eta_2 \hat{\Theta}_{f_2}(t) - \varrho_2 \varpi_2 \hat{\varepsilon}_2(t) \right] \\
 & \leq \mathcal{D}^\beta V_1(t) - k_2 e_2^2(t) - e_1(t)e_2(t) - x_1(t)e_2(t)e_3(t) \\
 & \quad - \frac{\eta_2}{2\varrho_2} \tilde{\Theta}_{f_2}^T(t) \tilde{\Theta}_{f_2}(t) \\
 & \quad + \frac{\eta_2}{2\varrho_2} \Theta_{f_2}^{*T} \Theta_{f_2}^* - \varpi_2 \mu_2 \tilde{\Theta}_{f_2}^T(t) \tilde{\Theta}_{f_2}(t) + \varpi_2 \tilde{\Theta}_{f_2}^T(t) \tilde{\varepsilon}_{f_2}(t) \\
 & \quad + \frac{1}{2}\zeta_2^2 + \frac{1}{2}\bar{\varepsilon}_2^2 \\
 & \leq -a_1 V_1(t) + e_1(t)e_2(t) + b_1 - k_2 e_2^2(t) - x_1(t)e_2(t)e_3(t) - \\
 & \quad e_1(t)e_2(t) + \frac{\eta_2}{2\varrho_2} \Theta_{f_2}^{*T} \Theta_{f_2}^* \\
 & \quad - \frac{\eta_2 + \varrho_2(2\varpi_2\mu_2 - 1)}{2\varrho_2} \tilde{\Theta}_{f_2}^T(t) \tilde{\Theta}_{f_2}(t) + \frac{1}{2} (\varpi_2 \bar{\varepsilon}_2 \psi_2 \tau_2)^2 \\
 & \quad + \frac{1}{2}\zeta_2^2 + \frac{1}{2}\bar{\varepsilon}_2^2 \\
 & \leq -a_2 V_2(t) - x_1(t)e_2(t)e_3(t) + b_2,
 \end{aligned} \tag{39}$$

where $a_2 = \min \{a_1, 2k_2, \eta_2 + \varrho_2(2\varpi_2\mu_2 - 1)\}$, $b_2 = b_1 + 0.5\varrho_2^{-1}\eta_2\|\Theta_{f_2}^*\|^2 + 0.5\varpi_2^2\bar{\varepsilon}_2^2\psi_2^2\tau_2^2 + 0.5\zeta_2^2 + 0.5\bar{\varepsilon}_2^2$.

Step 3. In virtue of Equations (3) and (7), we know

$$\mathcal{D}^\beta x_3(t) = \Theta_{f_3}^{*T} \Psi_{f_3}(\bar{\mathbf{x}}_3) + \varepsilon_{f_3}(t) + u_d(t) + x_1(t)x_2(t) - x_3(t). \tag{40}$$

On the basis of Equations (3) and (6), it is not difficult to check

$$\begin{aligned}
 \mathcal{D}^\beta e_3(t) & = \mathcal{D}^\beta x_3(t) - \mathcal{D}^\beta \alpha_{2,c}(t) \\
 & = \hat{\Theta}_{f_3}^T(t) \Psi_{f_3}(\bar{\mathbf{x}}_3) - \tilde{\Theta}_{f_3}^T(t) \Psi_{f_3}(\bar{\mathbf{x}}_3) + \varepsilon_{f_3}(t) + u_d(t) \\
 & \quad + x_1(t)x_2(t) - x_3(t) - \mathcal{D}^\beta \alpha_{2,c}(t).
 \end{aligned} \tag{41}$$

Configure the actual control law as

$$\begin{aligned}
 u_d(t) & = -k_3 e_3(t) + x_1(t)e_2(t) - \hat{\Theta}_{f_3}^T(t) \Psi_{f_3}(\bar{\mathbf{x}}_3) + x_3(t) \\
 & \quad - x_1(t)x_2(t) + \mathcal{D}^\beta \alpha_{2,c}(t),
 \end{aligned} \tag{42}$$

where k_3 is a given positive scalar.

By substituting Equation (42) into Equation (41), it is directly implied that

$$\mathcal{D}^\beta e_3(t) = -k_3 e_3(t) + x_1(t)e_2(t) - \tilde{\Theta}_{f_3}^T(t) \Psi_{f_3}(\bar{\mathbf{x}}_3) + \varepsilon_{f_3}(t). \tag{43}$$

Multiply both sides of Equation (43) by $e_3(t)$. Then according to Lemma 4, it follows that

$$\begin{aligned}
 & e_3(t)\mathcal{D}^\beta e_3(t) \\
 & \leq -k_3 e_3^2(t) + x_1(t)e_2(t)e_3(t) - e_3(t) \tilde{\Theta}_{f_3}^T(t) \Psi_{f_3}(\bar{\mathbf{x}}_3) + e_3(t) \varepsilon_{f_3}(t) \\
 & \leq -k_3 e_3^2(t) + x_1(t)e_2(t)e_3(t) - e_3(t) \tilde{\Theta}_{f_3}^T(t) \Psi_{f_3}(\bar{\mathbf{x}}_3) \\
 & \leq -k_3 e_3^2(t) + x_1(t)e_2(t)e_3(t) - e_3(t) \tilde{\Theta}_{f_3}^T(t) \Psi_{f_3}(\bar{\mathbf{x}}_3).
 \end{aligned} \tag{44}$$

Define a mapping $\mathbf{m}_3 : [0, +\infty) \rightarrow \mathbb{R}^{m \times m}$ by

$$\mathbf{m}_3(t) = \int_{t-\tau_3}^t \Psi_{f_3}(\bar{\mathbf{x}}_3(\tau)) \Psi_{f_3}^T(\bar{\mathbf{x}}_3(\tau)) d\tau$$

with $\tau_3 > 0$ being the length of an integral interval.

Inspired by the similar argument in Step 2, we construct the prediction error by

$$\hat{\varepsilon}_3(t) = \begin{cases} \mathbf{m}_3(t) \tilde{\Theta}_{f_3}(t) - \tilde{\varepsilon}_{f_3}(t), & t < T_{e_3} \\ \mathbf{m}_3(t) \tilde{\Theta}_{f_3}(T_{e_3}) - \tilde{\varepsilon}_{f_3}(T_{e_3}), & t \geq T_{e_3} \end{cases}$$

where $\tilde{\varepsilon}_{f_3} : [0, +\infty) \rightarrow \mathbb{R}^{m \times 1}$ is described as

$$\tilde{\varepsilon}_{f_3}(t) = \int_{t-\tau_3}^t \Psi_{f_3}(\bar{\mathbf{x}}_3(\tau)) \varepsilon_{f_3}(\tau) d\tau,$$

respectively. Let the IE condition be fulfilled, that is, $\mathbf{m}_3(t) \geq \mu_3 \mathbf{I}$ with a positive scalar μ_3 being the exciting strength, which implies $\Psi_{f_3}(\bar{\mathbf{x}}_3(t))$ is of IE on $t \in [T_{e_3} - \tau_3, T_{e_3}]$ for some $T_{e_3} > \tau_3$.

Introduce the adaptation law from composite learning as follows:

$$\mathcal{D}^\beta \hat{\Theta}_{f_3}(t) = \varrho_3 e_3(t) \Psi_{f_3}(\bar{\mathbf{x}}_3(t)) - \eta_3 \hat{\Theta}_{f_3}(t) - \varrho_3 \varpi_3 \hat{\varepsilon}_3(t) \tag{45}$$

with ϱ_3, η_3 , and ϖ_3 being positive design parameters.

To figure out the value of $\hat{\varepsilon}_3(t)$, let us define an auxiliary variable $\mathbf{H}_3(t)$ by

$$\mathbf{H}_3(t) = \mathbf{m}_3(t) \Theta_{f_3}^* + \tilde{\varepsilon}_{f_3}(t). \tag{46}$$

Equivalently, Equation (40) can be rewritten as

$$\Theta_{f_3}^{*T} \Psi_{f_3}(\bar{\mathbf{x}}_3) + \varepsilon_{f_3}(t) = \mathcal{D}^\beta x_3(t) - u_d(t) - x_1(t)x_2(t) + x_3(t). \tag{47}$$

Multiplying both sides of Equation (47) by $\Psi_{f_3}(\bar{\mathbf{x}}_3(t))$, we can see

$$\begin{aligned}
 & \Psi_{f_3}(\bar{\mathbf{x}}_3(t)) \left[\Psi_{f_3}^T(\bar{\mathbf{x}}_3(t)) \Theta_{f_3}^* + \varepsilon_{f_3}(t) \right] \\
 & = \Psi_{f_3}(\bar{\mathbf{x}}_3(t)) \left[\mathcal{D}^\beta x_3(t) - u_d(t) - x_1(t)x_2(t) + x_3(t) \right].
 \end{aligned} \tag{48}$$

From Equations (46) and (48), it is deduced that

$$\begin{aligned}
 \mathbf{H}_3(t) & = \int_{t-\tau_0}^t \Psi_{f_3}(\bar{\mathbf{x}}_3(\tau)) [\mathcal{D}^\beta x_3(\tau) - u_d(\tau) \\
 & \quad - x_1(\tau)x_2(\tau) + x_3(\tau)] d\tau.
 \end{aligned} \tag{49}$$

Thereby, calculating the accurate value of $\hat{\mathbf{e}}_3(t)$ leads to

$$\hat{\mathbf{e}}_3(t) = \mathbf{m}_3(t)\hat{\Theta}_{f_3}(t) - \mathbf{H}_3(t).$$

Select the candidate of Lyapunov function V_3 as the following formula:

$$V_3(t) = V_2(t) + \frac{1}{2}e_3^2(t) + \frac{1}{2\varrho_3}\tilde{\Theta}_{f_3}^T(t)\tilde{\Theta}_{f_3}(t). \quad (50)$$

In virtue of Lemma 4, taking the fractional derivative of Equation (50) implies

$$\begin{aligned} \mathcal{D}^\beta V_3(t) &= \mathcal{D}^\beta V_2(t) + \frac{1}{2}\mathcal{D}^\beta e_3^2(t) + \frac{1}{2\varrho_3}\mathcal{D}^\beta \tilde{\Theta}_{f_3}^T(t)\tilde{\Theta}_{f_3}(t) \\ &\leq \mathcal{D}^\beta V_2(t) + e_3(t)\mathcal{D}^\beta e_3(t) + \frac{1}{\varrho_3}\tilde{\Theta}_{f_3}^T(t)\mathcal{D}^\beta \tilde{\Theta}_{f_3}(t) \\ &= \mathcal{D}^\beta V_2(t) + e_3(t)\mathcal{D}^\beta e_3(t) + \frac{1}{\varrho_3}\tilde{\Theta}_{f_3}^T(t)\mathcal{D}^\beta \hat{\Theta}_{f_3}(t). \end{aligned} \quad (51)$$

Analogous to Equations (37) and (38), it is easily verified that

$$-\tilde{\Theta}_{f_3}^T(t)\hat{\Theta}_{f_3}(t) \leq -\frac{1}{2}\tilde{\Theta}_{f_3}^T(t)\tilde{\Theta}_{f_3}(t) + \frac{1}{2}\Theta_{f_3}^{*T}\Theta_{f_3}^*, \quad (52)$$

$$\varpi_3\tilde{\Theta}_{f_3}^T(t)\tilde{\mathbf{e}}_{f_3}(t) \leq \frac{1}{2}\tilde{\Theta}_{f_3}^T(t)\tilde{\Theta}_{f_3}(t) + \frac{1}{2}(\varpi_3\bar{\varepsilon}_3\psi_3\tau_3)^2, \quad (53)$$

in which $\psi_3 \geq \|\Psi_{f_3}(\bar{\mathbf{x}}_3(t))\|$ is a positive constant irrelevant with $\bar{\mathbf{x}}_3(t)$ and the number of neural nodes.

Synthesizing Equations (39), (44), (45), and (51)–(53) with Lemma 6, we arrive at

$$\begin{aligned} \mathcal{D}^\beta V_3(t) &\leq \mathcal{D}^\beta V_2(t) + e_3(t)\mathcal{D}^\beta e_3(t) \\ &+ \frac{1}{\varrho_3}\tilde{\Theta}_{f_3}^T(t) \left[\varrho_3 e_3(t)\Psi_{f_3}(\bar{\mathbf{x}}_3) - \eta_3\hat{\Theta}_{f_3}(t) - \varrho_3\varpi_3\hat{\mathbf{e}}_3(t) \right] \\ &\leq \mathcal{D}^\beta V_2(t) - k_3e_3^2(t) + x_1(t)e_2(t)e_3(t) - \frac{\eta_3}{2\varrho_3}\tilde{\Theta}_{f_3}^T(t)\tilde{\Theta}_{f_3}(t) \\ &+ \frac{\eta_3}{2\varrho_3}\Theta_{f_3}^{*T}\Theta_{f_3}^* - \varpi_3\mu_3\tilde{\Theta}_{f_3}^T(t)\tilde{\Theta}_{f_3}(t) + \varpi_3\tilde{\Theta}_{f_3}^T(t)\tilde{\mathbf{e}}_{f_3}(t) \quad (54) \\ &\leq -a_2V_2(t) - x_1(t)e_2(t)e_3(t) + b_2 - k_3e_3^2(t) + x_1(t)e_2(t)e_3(t) \\ &- \frac{\eta_3 + \varrho_3(2\varpi_3\mu_3 - 1)}{2\varrho_3}\tilde{\Theta}_{f_3}^T(t)\tilde{\Theta}_{f_3}(t) \\ &+ \frac{\eta_3}{2\varrho_3}\Theta_{f_3}^{*T}\Theta_{f_3}^* + \frac{1}{2}(\varpi_3\bar{\varepsilon}_3\psi_3\tau_3)^2 \\ &\leq -a_3V_3(t) + b_3, \end{aligned}$$

where $a_3 = \min\{a_2, 2k_3, \eta_3 + \varrho_3(2\varpi_3\mu_3 - 1)\}$, $b_3 = b_2 + 0.5\varrho_3^{-1}\eta_3\|\Theta_{f_3}^*\|^2 + 0.5\varpi_3^2\bar{\varepsilon}_3^2\psi_3^2\tau_3^2$.

By virtue of Equation (54) and Lemma 2, it is straightly examined that

$$\begin{aligned} V_3(t) &\leq V_3(0)E_\beta(-a_3t^\beta) + \frac{Mb_3}{a_3} \\ &\leq V_3(0)\frac{C}{1 + |-a_3t^\beta|} + \frac{Mb_3}{a_3} \quad (55) \\ &\leq V_3(0)C + \frac{Mb_3}{a_3}, \end{aligned}$$

for all $t \geq 0$, where $C \in \mathbb{R}^+$ is a certain constant, $M = \max\{1, C\}$. Therefore, $|e_i| \leq \sqrt{2(V_3(0)C + Mb_3/a_3)}$ and $\|\tilde{\Theta}_i\| \leq \sqrt{2\varrho_i(V_3(0)C + Mb_3/a_3)}$ for $i = 1, 2, 3$, which indicates $e_i, \tilde{\Theta}_i \in L_\infty$. This demonstrates the boundedness of the whole signals in the closed-loop system.

Given a sufficient small positive scalar $\epsilon = \epsilon_1 + \epsilon_2$ where $\epsilon_1 \geq \frac{Mb_3}{a_3}$ and $\epsilon_2 > 0$. By Equation (55), as $t \rightarrow \infty$, we have

$$0 < E_\beta(-a_3t^\beta) \leq \frac{C}{1 + a_3t^\beta} \rightarrow 0. \quad (56)$$

Based on Equations (55) and (56), if all design parameters are selected adequately, then there exists a certain $T > 0$ such that $E_\beta(-a_3t^\beta) \leq \epsilon_2$ whenever $t \geq T$ and hence $V_3(t) \leq \epsilon$. Consequently, the dynamic errors e_i and $\tilde{\Theta}_i$ converge toward a compact region of the origin, and the radius of the bounded region can be adjusted as small as possible.

Summarizing the above arguments, we obtain the following main result with respect to the system stability.

Theorem 1. Take into account the system Equation (3) with Assumption 1. Suppose that the control scheme comprises the virtual control functions Equations (10) and (27), the actual control law Equation (42), together with the composite learning laws (Equations 14, 45). Then, all the closed-loop signals are bounded, and the error variables $e_i, \tilde{\Theta}_i$ ($i = 1, 2, 3$) converge toward a small enough compact region of the origin.

Remark 1. In Xue et al. [8], a class of second-order command filter was extended into fractional form:

$$\begin{cases} \mathcal{D}^\beta v_1(t) = \varphi v_2(t), \\ \mathcal{D}^\beta v_2(t) = -2\lambda\varphi v_2(t) - \varphi(v_1(t) - \alpha(t)), \end{cases} \quad (57)$$

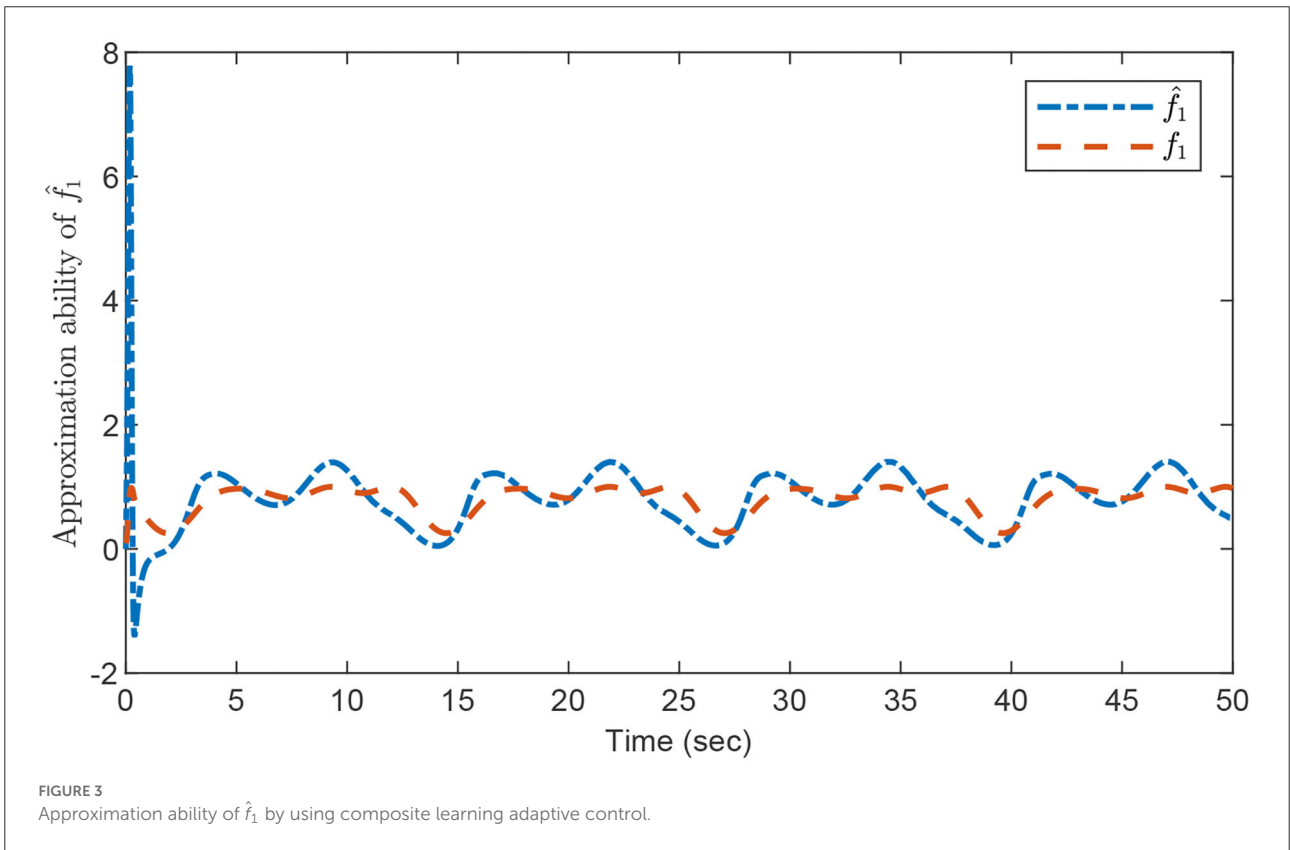
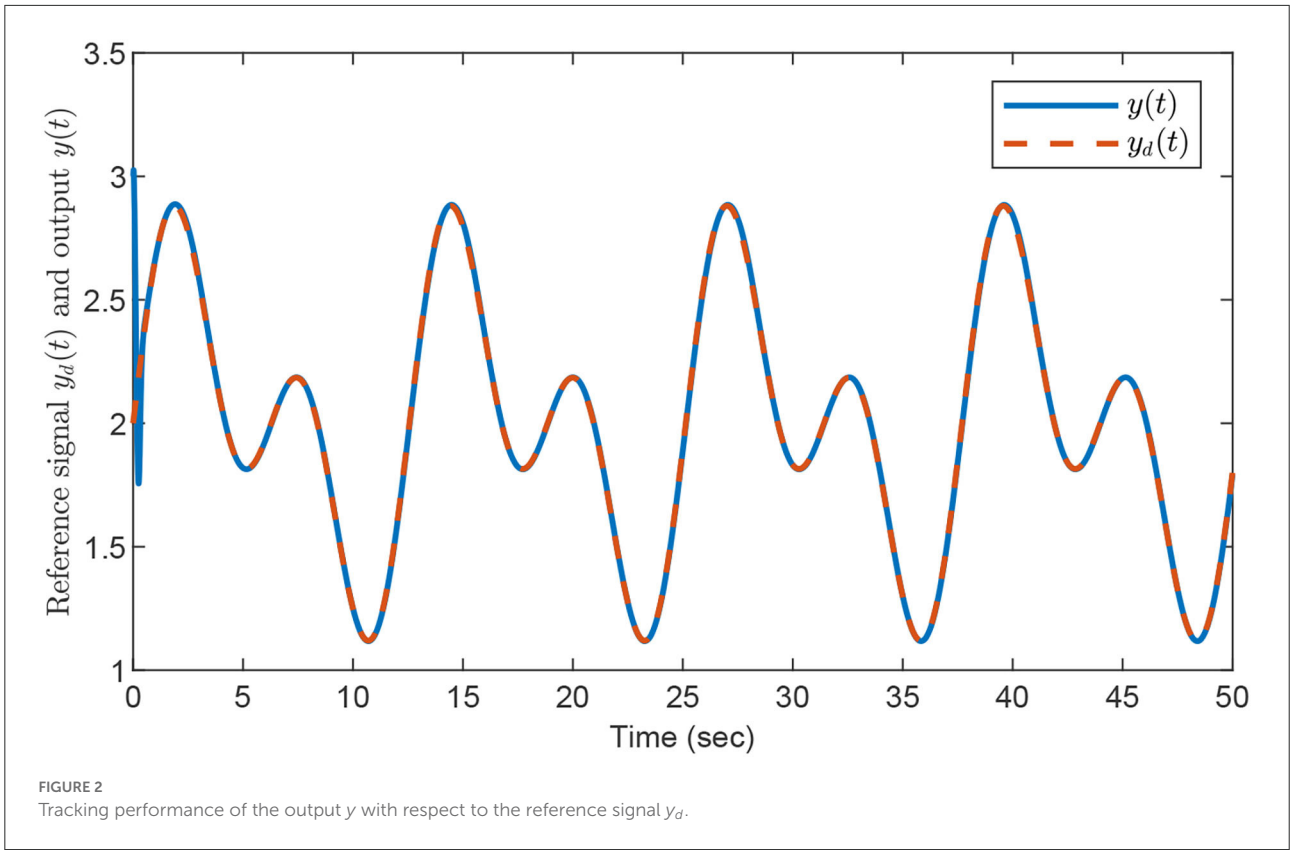
where $\alpha(t)$ is the filter input, $\varphi \in \mathbb{R}^+, \lambda \in [0, 1]$. The main advantage of Equation (57) is that its approximation accuracy for the input $\alpha(t)$ is much better than that of fractional-order dynamic surface (Equation 4) used in this paper. However, in contrast with Equation (57) which needs to satisfy that both $\mathcal{D}^\beta \alpha(t)$ and $\mathcal{D}^\beta \mathcal{D}^\beta \alpha(t)$ are bounded, Equation (4) only requires the boundedness of $\mathcal{D}^\beta \alpha(t)$ and shows less conservatism.

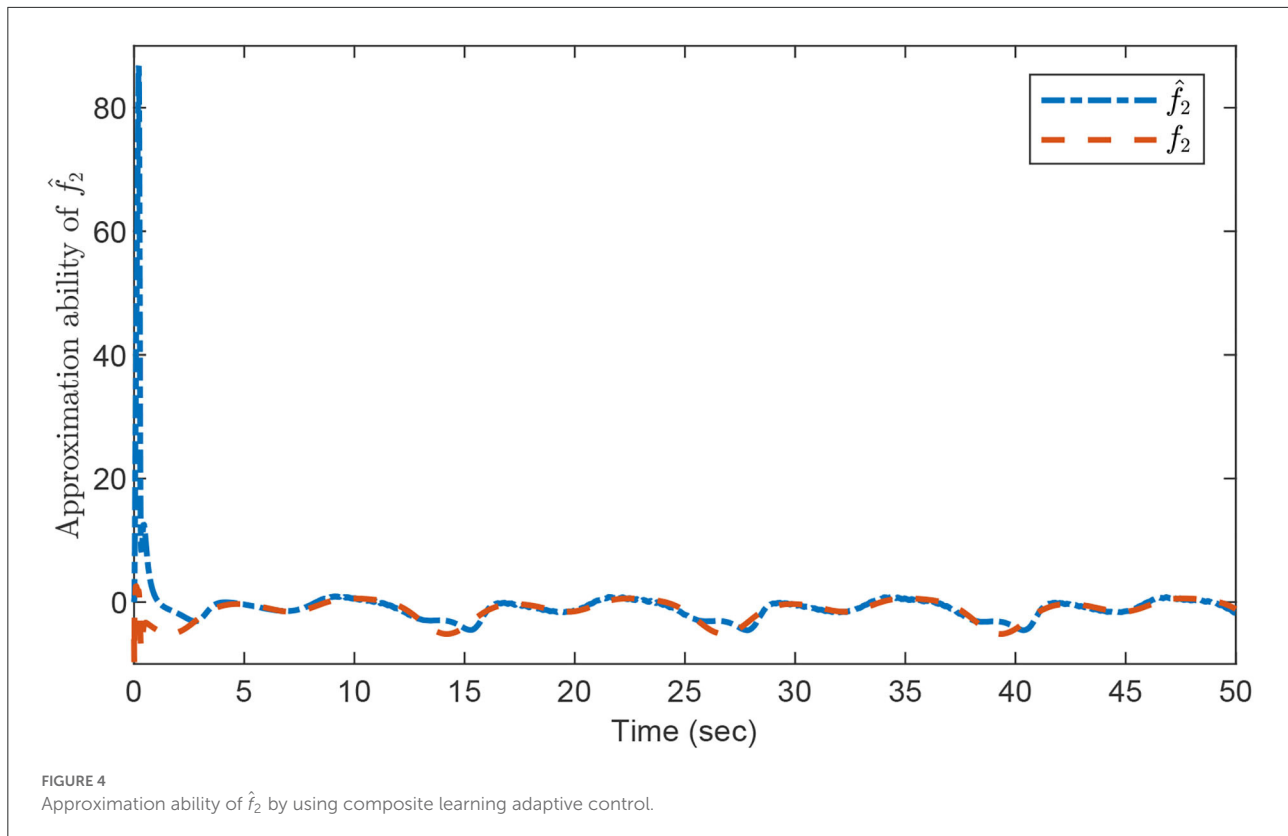
4. Simulation research

In this part, let us validate the efficiency of the proposed control scheme.

Pay attention to the practical model of fractional-order PMSM as follows:

$$\begin{cases} \mathcal{D}^\beta x_1(t) = f_1(\bar{\mathbf{x}}_1) + \sigma(x_2(t) - x_1(t)), \\ \mathcal{D}^\beta x_2(t) = f_2(\bar{\mathbf{x}}_2) + \gamma x_1(t) - x_1(t)x_3(t) - x_2(t), \\ \mathcal{D}^\beta x_3(t) = u_d(t) + x_1(t)x_2(t) - x_3(t), \end{cases} \quad (58)$$





where $\beta = 0.98$, $\sigma = 3$, $\gamma = 30$, $f_1(\bar{\mathbf{x}}_1) = \sin x_1$, and $f_2(\bar{\mathbf{x}}_2) = x_1 - x_2^2$ are unknown functions. The initial value of the full-state vector $\bar{\mathbf{x}}_3$ is considered as $\bar{\mathbf{x}}_3(0) = [3, 3, 3]^T$. Let the target signal be $y_d(t) = 2 + 0.5 \sin(0.5t) + 0.5 \sin(t)$.

Due to the uncertainty of f_1 and f_2 , we take advantage of three RBFNNs \hat{f}_1 and \hat{f}_2 in the simulation to approximate f_1 and f_2 , respectively. The single input of the first RBFNN \hat{f}_1 is x_1 , and the radial basis function is composed of twenty-one Gaussian functions which are uniformly distributed over the interval $[-2, 2]$. With respect to the second RBFNN \hat{f}_2 , we regard its input variables as x_1 and x_2 , and eight Gaussian functions evenly distributed on the interval $[-2, 2]$ are given for each input to induce the corresponding radial basis function. Thus, the number of all neural-network nodes related to \hat{f}_2 is selected as $8 \times 8 = 64$.

The design parameters are now selected as follows. First, let the input gain parameters are $k_1 = k_2 = k_3 = 15$. Second, the gain parameters of the dynamic surfaces are considered as $\varphi_1 = \varphi_2 = 80$. Third, set the integration duration to be $\tau_d = 15$ and the finalization time instants for IE to be $T_{e1} = T_{e2} = T_{e3} = 20$. At last, choose $\varrho_i = 30$ and $\eta_i = \varpi_i = 0.001$ with $i = 1, 2, 3$ for the composite learning adaptive control.

The relevant performance results are illustrated in Figures 2–4. Figure 2 shows that fast system response is

achieved and the output signal $y(t)$ can track the target trajectory $y_d(t)$ closely as desired. The approximation abilities of the estimations \hat{f}_i for f_i with $i = 1, 2$ via the designed composite learning algorithm are displayed in Figures 3, 4, respectively. By using the introduced composite learning adaptive control method under the IE condition, one can observe that excellent estimation preciseness is obtained, which confirms the robustness of the introduced composite learning neural control approach as well as its powerful capability of chaos suppression.

5. Conclusion

In the article, the tracking control of fractional-order PMSMs is studied by establishing an adaptive backstepping composite learning neural control scheme. Neural networks are applied to serve as functional approximations, and a composite learning adaptive control algorithm is constructed to guarantee the high estimation accuracy of adaptation parameters. Employing the extended Lyapunov stability criterion, it is proven that the proposed control method achieves robust control performance and plays a vital role in tackling the tracking control problem of uncertainty fractional-order

PMSMs. The simulation example reveals that the provided control method can improve the tracking efficiency. In future, we will focus on the study of fractional permanent magnet motor system with complicated characteristics of control input, such as input saturation, input dead-zone, and input delay.

Author contributions

CW: conceptualization, methodology, formal analysis, investigation, validation, software, data curation, and writing.

Funding

This work was supported by the National Natural Science Foundation of China (Grant No. 11302184), the Fujian Provincial Natural Science Foundation (Grant No. 2021J011194), and Research Climbing Program of Xiamen University of Technology (Grant No. XPDQK20020).

References

- Miller KS, Ross B. *An Introduction to the Fractional Calculus and Fractional Differential Equations*. New York, NY: Wiley-Interscience Publication (1993).
- Podlubny I. *Fractional Differential Equations*. New York, NY: Academic Press (1999).
- Aguila-Camacho N, Duarte-Mermoud MA, Gallegos JA. Lyapunov functions for fractional order systems. *Commun Nonlinear Sci Num Simulat.* (2014) 19:2951–7. doi: 10.1016/j.cnsns.2014.01.022
- Gong P. Distributed tracking of heterogeneous nonlinear fractional-order multi-agent systems with an unknown leader. *J Franklin Inst.* (2017) 354:2226–44. doi: 10.1016/j.jfranklin.2017.01.001
- Han SI. Fractional-Order command filtered backstepping sliding mode control with fractional-order nonlinear disturbance observer for nonlinear systems. *J Franklin Inst.* (2020) 357:6760–76. doi: 10.1016/j.jfranklin.2020.04.055
- Liu H, Pan Y, Cao J, Zhou Y, Wang H. Positivity and stability analysis for fractional-order delayed systems: a T-S fuzzy model approach. *IEEE Trans Fuzzy Syst.* (2021) 29:927–39. doi: 10.1109/TFUZZ.2020.2966420
- Song S, Park JH, Zhang B, Song X. Observer-based adaptive hybrid fuzzy resilient control for fractional-order nonlinear systems with time-varying delays and actuator failures. *IEEE Trans Fuzzy Syst.* (2021) 29:471–85. doi: 10.1109/TFUZZ.2019.2955051
- Xue G, Lin F, Li S, Liu H. Adaptive fuzzy finite-time backstepping control of fractional-order nonlinear systems with actuator faults via command-filtering and sliding mode technique. *Inf Sci.* (2022) 600:189–208. doi: 10.1016/j.ins.2022.03.084
- Li Z, Park JB, Joo YH, Zhang B, Chen G. Bifurcations and chaos in a permanent-magnet synchronous motor. *IEEE Trans Circ Syst I Fundament Theory Appl.* (2002) 49:383–7. doi: 10.1109/81.989176
- Yu J, Chen B, Yu H, Gao J. Adaptive fuzzy tracking control for the chaotic permanent magnet synchronous motor drive system via backstepping. *Nonlinear Anal.* (2011) 12:671–81. doi: 10.1016/j.nonrwa.2010.07.009
- Yang X, Yu J, Wang QG, Zhao L, Yu H, Lin C. Adaptive fuzzy finite-time command filtered tracking control for permanent magnet synchronous motors. *Neurocomputing.* (2019) 337:110–9. doi: 10.1016/j.neucom.2019.01.057
- Zhou S, Sui S, Tong S. Adaptive neural networks optimal control of permanent magnet synchronous motor system with state constraints. *Neurocomputing.* (2022) 504:132–40. doi: 10.1016/j.neucom.2022.06.114
- Basin M, Rodriguez-Ramirez P, Ramos-Lopez V. Continuous fixed-time convergent controller for permanent-magnet synchronous motor with unbounded perturbations. *J Franklin Inst.* (2020) 357:11900–13. doi: 10.1016/j.jfranklin.2019.11.059
- Gil J, You S, Lee Y, Kim W. Nonlinear sliding mode controller using disturbance observer for permanent magnet synchronous motors under disturbance. *Expert Syst Appl.* (2023) 214:119085. doi: 10.1016/j.eswa.2022.119085
- Li C, Yu S, Luo X. Fractional-order permanent magnet synchronous motor and its adaptive chaotic control. *Chin Phys B.* (2012) 21:168–73. doi: 10.1088/1674-1056/21/10/100506
- Xue W, Li Y, Cang S, Jia H, Wang Z. Chaotic behavior and circuit implementation of a fractional-order permanent magnet synchronous motor model. *J Franklin Inst.* (2015) 352:2887–98. doi: 10.1016/j.jfranklin.2015.05.025
- Lu S, Wang X, Li Y. Adaptive neural network finite-time command filtered tracking control of fractional-order permanent magnet synchronous motor with input saturation. *J Franklin Inst.* (2020) 357:13707–33. doi: 10.1016/j.jfranklin.2020.10.021
- Zhang S, Wang C, Zhang H, Ma P, Li X. Dynamic analysis and bursting oscillation control of fractional-order permanent magnet synchronous motor system. *Chaos Solit Fractals.* (2022) 156:111809. doi: 10.1016/j.chaos.2022.111809
- Sanner RM, Slotine JJE. Gaussian networks for direct adaptive control. *IEEE Trans Neural Netw.* (1992) 3:837–63. doi: 10.1109/72.165588
- Kurdila AJ, Narcowich FJ, Ward JD. Persistency of excitation in identification using radial basis function approximants. *SIAM J Control Optim.* (2006) 33:625–42. doi: 10.1137/S0363012992232555
- Wang C, Hill DJ. Learning from neural control. *IEEE Trans Neural Netw.* (2006) 17:130–46. doi: 10.1109/TNN.2005.860843
- Wang C, Wang M, Liu T, Hill DJ. Learning from ISS-modular adaptive NN control of nonlinear strict-feedback systems. *IEEE Trans Neural Netw Learn Syst.* (2012) 23:1539–50. doi: 10.1109/TNNLS.2012.2205702

Acknowledgments

The author would like to convey his acknowledgments to the editors and the reviewers for their helpful comments and recommendations.

Conflict of interest

The author declares that the research was conducted in the absence of any commercial or financial relationships that could be construed as a potential conflict of interest.

Publisher's note

All claims expressed in this article are solely those of the authors and do not necessarily represent those of their affiliated organizations, or those of the publisher, the editors and the reviewers. Any product that may be evaluated in this article, or claim that may be made by its manufacturer, is not guaranteed or endorsed by the publisher.

23. Wang M, Wang C, Liu X. Dynamic learning from adaptive neural control with predefined performance for a class of nonlinear systems. *Inf Sci.* (2014) 279:874–88. doi: 10.1016/j.ins.2014.04.038
24. Pan Y, Yu H. Biomimetic hybrid feedback feedforward neural-network learning control. *IEEE Trans Neural Netw Learn Syst.* (2017) 28:1481–7. doi: 10.1109/TNNLS.2016.2527501
25. Pan Y, Sun T, Liu Y, Yu H. Composite learning from adaptive backstepping neural network control. *Neural Network.* (2017) 95:134–42. doi: 10.1016/j.neunet.2017.08.005
26. Xu B, Sun F, Pan Y, Chen B. Disturbance observer based composite learning fuzzy control of nonlinear systems with unknown dead zone. *IEEE Trans Syst Man Cybern Syst.* (2017) 47:1854–62. doi: 10.1109/TSMC.2016.2562502
27. Liu H, Pan Y, Cao J. Composite learning adaptive dynamic surface control of fractional-order nonlinear systems. *IEEE Trans Cybern.* (2020) 50:2557–67. doi: 10.1109/TCYB.2019.2938754
28. Guo Y, Qin H, Xu B, Han Y, Fan QY, Zhang P. Composite learning adaptive sliding mode control for AUV target tracking. *Neurocomputing.* (2019) 351:180–6. doi: 10.1016/j.neucom.2019.03.033
29. Guo K, Pan Y, Zheng D, Yu H. Composite learning control of robotic systems: a least squares modulated approach. *Automatica.* (2020) 111:108612. doi: 10.1016/j.automatica.2019.108612
30. Xue G, Lin F, Li S, Liu H. Composite learning control of uncertain fractional-order nonlinear systems with actuator faults based on command filtering and fuzzy approximation. *Int J Fuzzy Syst.* (2022) 24:1839–58. doi: 10.1007/s40815-021-01242-3